

Inner-shell excitation probabilities in intermediate-heavy, asymmetric ion-atom collisions

D. Maor,* D. Liesen, and P. H. Mokler

Gesellschaft für Schwerionenforschung, D-6100 Darmstadt, Federal Republic of Germany

B. Rosner

Department of Physics, Technion, 32000 Haifa, Israel

H. Schmidt-Böcking†

Institut für Kernphysik, Universität Frankfurt, D-6000 Frankfurt, Federal Republic of Germany

R. Schuch

Physikalisches Institut der Universität Heidelberg, D-6900 Heidelberg, Federal Republic of Germany

(Received 14 April 1982)

The impact-parameter dependence of the inner-shell excitation was measured for 1.4-MeV/u Ni ions on Zr, Ag, Te, and Au. All the measured vacancy-production probabilities have impact-parameter dependences typical for direct excitation. Scaling the impact parameter with the adiabatic radius, calculated using united-atom binding energies, all Ni K data can be brought to one common curve. The impact-parameter region contributing most to the vacancy-production cross section, as well as the plateau value of the vacancy-production probability attained at the lowest impact parameters could be explained by extending the semiclassical-approximation method to these collision systems.

I. INTRODUCTION

Various mechanisms may contribute to the inner-shell excitation in heavy-ion-atom collisions (for a review see, e.g., Refs. 1 and 2). A useful approach for separating these mechanisms is to measure the inner-shell vacancy-production probability $P(b)$ as a function of the impact parameter b , since the shape of this function may be quite different for the different mechanisms.

Two types of inner-shell vacancy-production mechanisms have been treated theoretically in detail, the direct excitation and the molecular-orbital promotion.

For very asymmetric collision systems ($Z_P \ll Z_T$), the inner-shell target electrons have a certain probability of being ejected due to the (small) perturbation of the potential caused by the projectile. This excitation to the continuum called direct excitation has been treated by several perturbation-theory approaches.^{1,2}

In nearly symmetric systems ($Z_P \approx Z_T$), electron promotion via molecular orbitals has been found to be the main inner-shell vacancy-production

mechanism, when the collision velocity v is much smaller than the electron velocity u in the relevant orbital. In particular, K-hole production is attributed to promotion via the $2p\sigma - 2p\pi$ rotational coupling. This has been confirmed experimentally for symmetric and nearly symmetric systems with $Z_P + Z_T \lesssim 70$.

For very heavy systems ($Z_P + Z_T \gtrsim 130$), direct excitation is found to dominate even in nearly symmetric systems.^{3,4}

In the region which is intermediary, regarding the asymmetry of the collision ($0.3 \lesssim Z_P/Z_T < 1$), the united-atomic number ($60 < Z_{UA} = Z_P + Z_T < 130$), and the collision velocity ($0.1 \lesssim v/u \lesssim 0.4$), neither perturbation theory nor the molecular-orbital (MO) model are necessarily appropriate. Here the inner-shell excitation mechanism is still not well known.

The problem of theoretically evaluating the direct excitation contribution in this region has been approached from both sides, by extension of the semiclassical-approximation (SCA) perturbation theory by Andersen *et al.*⁵ and by the use of the molecular-orbital model by Briggs.⁶ For this intermediate collision region the contribution from elec-

tron promotion, e.g., via $2p\sigma - 2p\pi$ rotational coupling, cannot be calculated precisely enough from scaling laws⁷ whose range of validity has been confirmed experimentally to the low- Z regime.⁸

The aim of the present work is to investigate the mechanisms involved in the inner-shell vacancy production in this intermediate region with varying asymmetry ($Z_P = 28$; $28 \leq Z_T \leq 79$; $0.1 \leq v/u \leq 0.4$) and to test the applicability of the above-mentioned models in these cases.

II. EXPERIMENTAL ARRANGEMENT

The measurements were performed using the UNILAC at the Gesellschaft für Schwerionenforschung, Darmstadt. A well-collimated beam of Ni^{16+} ions at 1.4 MeV/u impinged at 45° upon solid targets of Ni, Zr, Ag, Te, and Au. The targets were 25 to 60 $\mu\text{g}/\text{cm}^2$ thick on 15- $\mu\text{g}/\text{cm}^2$ carbon backing, the Au target was self-supporting and 90 $\mu\text{g}/\text{cm}^2$ thick. The x rays were detected with a Si(Li) detector positioned at 90° to the beam. A 50- $\mu\text{g}/\text{cm}^2$ -thick aluminium absorber reduced the intensity of the low-energy x rays (1–3 keV). The scattered projectiles were detected by a radially position-sensitive, parallel-plate avalanche detector,⁹ which was positioned during the experiment at two different distances from the target, to enable detection of particles scattered to laboratory angles of 0.5° to 36° . The impact parameters were calculated assuming an exponentially screened Coulomb potential: $V(r) = (Z_1 Z_2 e^2 / r) e^{-r/R_0}$ with

$$R_0 = 0.885a_0 (Z_1^{2/3} + Z_2^{2/3})^{-1/2}$$

(a_0 is the Bohr radius). The screening correction is less than 20% for the smallest scattering angles measured in the experiment.

K x rays of Ni as well as K x rays of Zr and L x rays of Te and Au were recorded in coincidence with the scattered particles on a PDP computer, in event mode, using standard coincidence techniques. The ratio of the true- to random-coincidence events was typically 10:1.

The absolute value of the vacancy-production probability per shell i at a scattering angle θ is determined by

$$P_i(\theta) = n_{\text{tr}}^i(\theta) / n_s(\theta) (\omega_x^i \epsilon_x^i \Delta\Omega_x)^{-1}, \quad (1)$$

where $n_{\text{tr}}^i(\theta)$ is the number of true coincidences, $n_s(\theta)$ the number of detected scattered particles, ω_x^i the fluorescence yield of shell i , and $\epsilon_x^i \Delta\Omega_x$ are the corresponding efficiency and solid angle of the

detector.

It is seen from Eq. (1) that in addition to the statistical uncertainty in $n_{\text{tr}}^i(\theta)$ and $n_s(\theta)$, only the uncertainties in fluorescence yield and in the efficiency and solid angle of the Si(Li) detector will contribute to the uncertainty in $P_i(\theta)$.

The efficiency ϵ_x^i was calculated using the measured thickness of the absorber as well as the Be-window, Au-contact, and Si-deadlayer thicknesses given by the manufacturer; the attenuation coefficients from Storm and Israel¹⁰ were used. $\Delta\Omega_x$ was determined geometrically. The overall uncertainty in $\epsilon_x \Delta\Omega_x$ is estimated to be about 20%.

Neutral-atom fluorescence yields are known to underestimate the realistic values in heavy-ion collisions, due to the multiple outer-shell ionization accompanying the inner-shell vacancy production. In the data reduction performed here, a procedure described, for instance, by Greenberg *et al.*¹¹ has been used to estimate all K -shell fluorescence yields. These values are listed in Table I and are assumed to be correct within a relative accuracy of $\pm 20\%$. More problematic is the fluorescence yield for the gold L shell, however, recent measurements and calculations by Schönfeldt *et al.*¹² for $\text{Pb} \rightarrow \text{Ni}$ at the same collision velocity indicate that an average fluorescence yield of about 0.5 could be assumed within the above-stated accuracy.

III. DATA ANALYSIS AND DISCUSSION

A. Data

Figure 1 presents in a semilogarithmic plot the vacancy-production probability $P(b)$ for the Ni K and Zr K shells in the collision $\text{Ni} \rightarrow \text{Zr}$. The gen-

TABLE I. Fluorescence yields used in the present analysis for bombardment with Ni ions of energy E .

E (MeV)	Target	ω_{Ni}	ω_{target}
45	Mn	0.52	0.39
94	Mn	0.58	0.44
138	Mn	0.60	0.45
54	Ni	0.53	0.53
90	Ni	0.58	0.58
54	Ge	0.53	0.63
90	Ge	0.58	0.68
54	Rb	0.53	0.72
90	Rb	0.58	0.76
83	Zr	0.57	0.78
83	Ag, Te	0.57	
83	Au	0.57	0.50 (L shell)

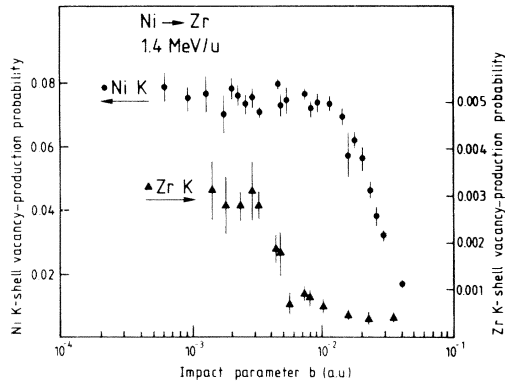


FIG. 1. Vacancy-production probabilities for Ni K and Zr K in the Ni→Zr collision, as a function of impact parameter.

eral shape of the $P(b)$ curves, i.e., an increase in the probability with decreasing impact parameter, until a plateau value P^* is reached, is typical for all Ni K curves in the asymmetric systems, as well as for Zr K and Au L. There is no indication of an adiabatic peak which is the typical feature of rotational coupling, although the projectile velocity v is such that for all atomic shells mentioned above the adiabaticity parameter $\eta = v^2/u^2$ is below 0.2.

Only the symmetric Ni→Ni system displays a shape typical for rotational coupling. Some structure is also found in the Te L data, which was the least-bound orbital investigated. These results have already been reported.¹³ Schuch *et al.* also published $P(b)$ data for Ni→Ni at a slightly higher energy (1.55 MeV/u). There is good agreement between the two sets of data. Schuch *et al.* also present $P(b)$ values for Ni K in Ni→Ge and Ni→Rb. There one can see the decrease in the prominence of the adiabatic peak with increasing asymmetry preceding its complete disappearance in the more asymmetric systems investigated here.

The $P(b)$ curves in the systems we report here have the typical shape of a direct-excitation process—a flat plateau and a steep falloff at a certain impact parameter.¹⁴ Such a direct-excitation process has also been postulated in more symmetric collision systems, where it seems to be responsible for the filling up of the valley between the adiabatic and kinematic peaks which are typical for rotational coupling (see, e.g., Ref. 15).

B. Vacancy sharing

Before the data are analyzed with respect to this direct-excitation process, we have to consider a pos-

sible transfer of vacancies by long-range radial coupling between close-lying orbitals, often called vacancy sharing.

In Fig. 2, schematic correlation diagrams of the five collision systems investigated are shown. According to these diagrams, radial couplings at relatively large internuclear distances are important for the following pairs of orbitals: $1s\sigma$ - $2p\sigma$ coupling for Ni on Zr and $2p\sigma$ - $3d\sigma$ coupling for Ni on Te and Ni on Au.

The integral vacancy-sharing ratios can be obtained from the singles x-ray spectra, if we assume that the vacancy-sharing contribution is the dominant one for the total vacancy-production cross section of the more strongly bound level. This is justified by the fact that the radial coupling is active up to very large impact parameters compared with the direct excitation. The regions for sharing and direct excitation are spatially separated; vacancy sharing occurs only on the outgoing part of the collision at large internuclear distances.

The sharing ratio w_{ij} of the more strongly bound shell i to the less strongly bound shell j is then given by

$$w_{ij} = \frac{n_x^i \omega_x^j \epsilon_x^j}{n_x^j \omega_x^i \epsilon_x^i}, \quad (2)$$

where n_x^i and n_x^j are the singles spectra yields of the corresponding shells. Therefore, the integral sharing ratio can be determined primarily to the accuracy to which the fluorescence yield ratio is known.

For the $1s\sigma$ - $2p\sigma$ coupling in Ni on Zr we obtain experimentally $w = 8.4 \times 10^{-3}$, in good agreement with the calculated value of 7.5×10^{-3} according to Meyerhof.¹⁶ For the $2p\sigma$ - $3d\sigma$ coupling we obtain for Ni K—Te L a vacancy sharing of $w = 2.2 \times 10^{-2}$ and for Au L—Ni K a vacancy sharing of $w = 0.42$. This very large last value agrees qualitatively with

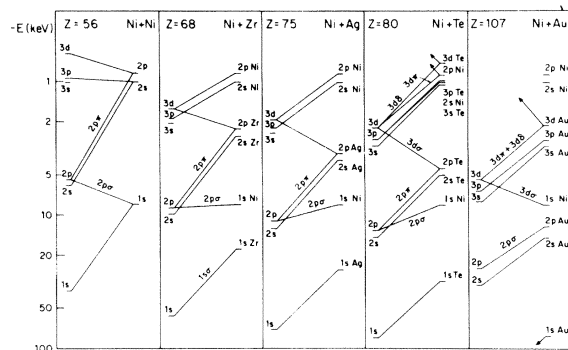


FIG. 2. Schematic correlation diagrams for the investigated collision systems.

the predictions of Fritsch and Wille¹⁷ for swapped systems (systems in which the L shell of the heavier collision partner is more strongly bound than the K shell of the lighter collision partner).

We can compare these integral values with the vacancy-production probability ratios obtained at the relatively small impact parameters investigated. Figure 3 displays the impact-parameter dependence of the ratio $P(b)_{ZrK}/P(b)_{NiK}$. The broken line indicates the integral ratio obtained from the total cross sections. The ratios for the larger impact parameters are relatively constant and agree with the integral ratio. Since the one-way-passage vacancy sharing is known to be largely impact-parameter independent in the relevant impact-parameter region we may, to a reasonable accuracy, take the integral ratio as the constant value for vacancy sharing in the whole b region of interest here. The increase in the vacancy-production probability ratio at the smaller impact parameters seen in Fig. 3 is hence attributed to direct excitation in the lower level, here the $1s\sigma$ level.

A similar picture is obtained if one plots the vacancy-production ratios for the other two pairs of sharing orbitals. At the largest impact parameters, the differential ratios are in accordance with the integral ones, and at lower impact parameters the ratio increases. The impact parameters at which this increase takes place are different in the different systems and reflect the respective increase in $P(b)$ for the lower MO at small internuclear distances due to the onset of the direct-excitation mechanism.

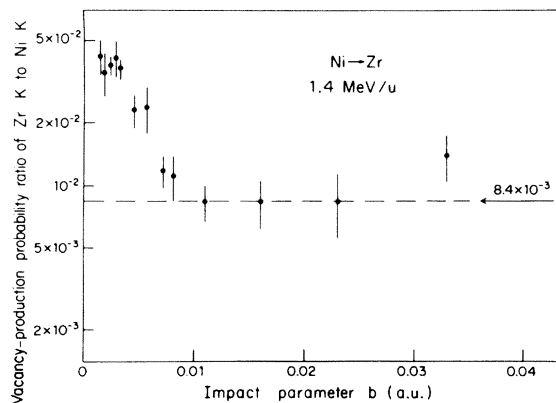


FIG. 3. Vacancy-production probability ratio of Zr K to Ni K in the Ni→Zr collision as a function of impact parameter. Broken line and the value above the arrow designate the total vacancy-production cross-section ratio.

C. Direct excitation

The shapes of the $P(b)$ curves do not display the features typical for $2p\sigma$ - $2p\pi$ or $3d\sigma$ - $3d\pi$ rotational coupling (cf. Sec. IIIA) which should manifest themselves mainly in the appearance of the so-called “adiabatic peak.”^{7,18} This obvious reduction of the rotational-coupling contribution is probably due to the diminishing number of vacancies n_{π_x} in the $2p\pi$ or $3d\pi$ orbitals which have to be formed on the incoming part of the collision; n_{π_x} decreases with increasing binding energy of the target $2p$ or $3d$ orbital, respectively. On the other hand, the decrease of the rotational coupling probability in heavier systems because of relativistic effects, i.e., mainly because of the increase in the splitting of the $2p_{1/2}$ and $2p_{3/2}$ levels in the united-atomic system, has been shown to be small.¹⁹

However, regardless of the disappearance of the rotational coupling, the vacancy-production probabilities remain very high. For example, a vacancy-production probability of about 8% is obtained for the Ni K shell in Ni→Zr at small impact parameters (cf. Fig. 1). It will be shown below that this high excitation probability can indeed be explained within the framework of direct excitation.

The shape of such a curve is again displayed in Fig. 4, for Ni K in the system Ni on Te on a linear-linear scale. The displayed $P_r(b)$ values (●) are obtained from the measured $P(b)$ data, after subtrac-

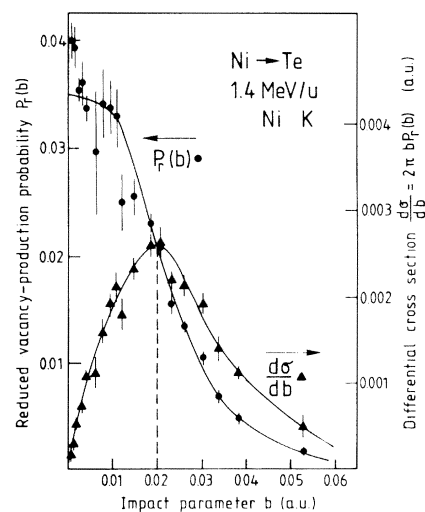


FIG. 4. Reduced vacancy-production probability $P_r(b)$, obtained after the subtraction of the vacancy-sharing contribution, for Ni K in the collision Ni→Te, as well as the corresponding differential cross section, as a function of impact parameter.

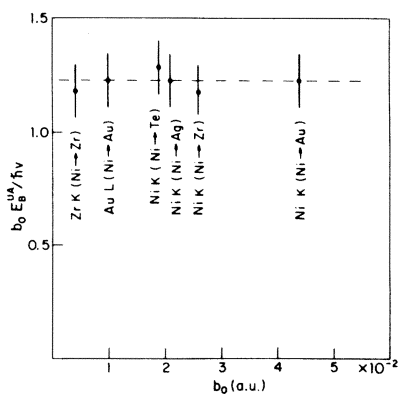


FIG. 5. Plot of the quantity $b_0 E_B^{UA} / \hbar v$ as a function of b_0 . The broken line gives the average value of the displayed data points.

tion of the vacancy-sharing contribution, as explained in Sec. III A. A second set of data points (\blacktriangle) in Fig. 4 displays the differential cross section

$$\frac{d\sigma}{db} = 2\pi b P_r(b) \quad (3)$$

which indicates the relative contribution to the total vacancy-production cross section from a certain impact parameter b . Both curves are similar in shape to SCA calculations (cf. Refs. 5, 14, and 20). Of course, SCA calculations cannot generate the exact $P(b)$ curve for these heavy projectiles, even if the assumption that the vacancy production is due to direct excitation is correct, because the SCA is a perturbation-theory method, which assumes the projectile to be a relatively small perturbation on the target. However, one feature of the direct excitation should be in these systems also. The impact parameter at which $d\sigma/db$ reaches its maximum value should be approximately equal to the adiabatic radius given by

$$r_{\text{ad}} \equiv \frac{\hbar v}{\Delta E}, \quad (4)$$

where v is the collision velocity and ΔE is the difference in energies between the final and initial state of the excited electron. The correctness of the above statement outside the range of validity of the SCA is shown mathematically in Refs. 14 and 21. Physically, the adiabatic radius is just the inverse of the minimal momentum transfer q_0 to the electron compatible with an energy transfer ΔE .

For collisions with very light projectiles it is known that the dominant direct excitation takes place to states near the continuum boundary.¹⁴ The

same seems to be valid also for $1s\sigma$ excitation in very heavy projectile collisions.^{3,4} Therefore, the value ΔE in Eq. (4) can be replaced by the binding energy E_B of the level from which the excitation takes place.

In our measured $P(b)$ curves for Ni K in the four asymmetric systems, we find that the impact parameter b_0 at which $bP(b)$ has its maximum is not constant. It decreases from Ni \rightarrow Zr through Ni \rightarrow Ag to Ni \rightarrow Te and then drastically increases for Ni \rightarrow Au.

Considering the fact that the adiabaticity parameter η is of the order of 0.1 for the Ni K shell, one can assume that the binding energy of these electrons can follow the MO energy curves. It can be seen from Fig. 2 that indeed the behavior of the binding energy of the MO to which the Ni K orbital correlates ($2p\sigma$ for the first three systems and $3d\sigma$ for Ni \rightarrow Au), is in qualitative agreement with the above-mentioned changes in b_0 .

Since the values of b_0 are of the order of a few times 10^{-2} a.u., where the changes in the MO binding energies relative to the united atom are not large any more, we can compare the experimental b_0 values with adiabatic radii calculated with united-atom binding energies. Following Ref. 22 we do that by writing

$$b_0 = C r_{\text{ad}}^{\text{UA}} \equiv C \frac{\hbar v}{E_B^{\text{UA}}}, \quad (5)$$

where C should be a constant of the order of unity.

This assumption is tested in Fig. 5 where the quantity $b_0 E_B^{\text{UA}} / \hbar v$ is plotted vs b_0 . The figure also includes the values for the Zr K and Au L shells for

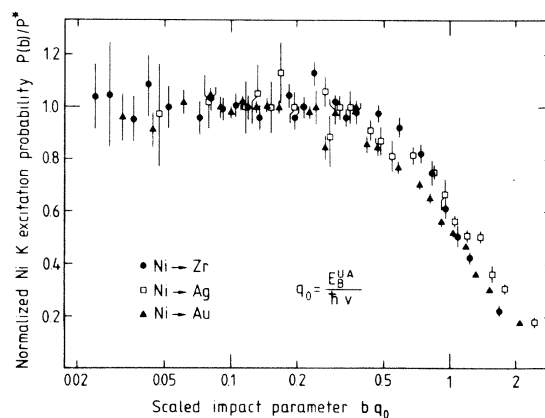


FIG. 6. Vacancy-production probability for the Ni K shell normalized to its plateau value at low impact parameters vs the impact parameter scaled with the united-atom adiabatic radius $r_{\text{ad}}^{\text{UA}} = 1/q_0$, for the collision systems Ni \rightarrow Zr, Ag, Au.

which the adiabaticity parameter is even smaller than for NiK. It is seen that the data are indeed consistent with a constant value within the experimental uncertainty, yielding $C = 1.23 \pm 0.05$. This value is intermediate between $C = 1.78$ calculated for very asymmetric and light systems ($Z_1 + Z_2 < 50$) (Ref. 14) and $C = 0.8 \pm 0.1$ for $2p_{1/2}\sigma$ ionization in Pb on Pb at 3–6 MeV/u.²²

Previous $P(b)$ measurements performed in gaseous S→Kr and S→Xe systems under single collision conditions²³ yield values of $C \sim 1.4$. This seems again to fit in the systematics indicated above; however, it should be stressed that no theoretical calculations of C in these medium-heavy systems are available.

In order to test the similarity of the whole $P(b)$ curve for NiK in the different systems, we have plotted in Fig. 6 the vacancy-production probability in each collision system in units of its respective plateau value at small b , P^* , as a function of the impact parameter in units of the respective calculated united-atom adiabatic radius. We see that the data points for the three collision systems Ni→Zr, Ni→Ag, and Ni→Au form one common curve.

The Ni→Te data (not displayed) contain, as mentioned before, a sharing contribution from the above-lying TeL shell. If, however, we consider the reduced $P_r(b)$ values obtained after the subtraction of the sharing contribution (see Fig. 4), they would also fall on the same universal curve.

Considering now the vacancy-production probabilities at the plateau $P^* = P(b \sim 0)$ we try to compare the experimental values obtained here and elsewhere,^{8,24} with two theoretical approaches, extended to these collision systems: (i) The SCA scaling for heavier projectiles as applied by Andersen *et al.*⁵ for quite asymmetric systems ($Z_P/Z_T \leq 0.25$) and (ii) the procedure outlined by Briggs⁶ for symmetric systems and extended by Meyerhof for the case of the ionization of the $3d\sigma$ MO.^{25,26}

In both calculations $P(b)$ depends sensitively on the binding energy of the electron. A 10% change in E_B can change $P(b \sim 0)$ easily by more than a factor of 2. Because of the high ionization of the projectile in a solid, the screening from outer electrons is reduced and the electron binding energy may increase by about 2 keV relative to neutral-atom values.¹² Also, in these not fully adiabatic collisions, it is difficult to define the correct frame of reference for the participating electrons and therefore the correct velocity of the perturbing potential. In addition, two factors mentioned before introduce inaccuracies in the experimental values,

namely, the fluorescence yield for these highly ionized atoms and the subtraction of the vacancy-sharing contribution.

Taking into account all above uncertainties, an agreement between the absolute values of P_{expt}^* and P_{calc}^* within better than a factor of 2 cannot be expected. Therefore, the relative dependence of P^* on E_B^{UA} and v should be a more sensitive test of an interpretation of the experimental results in terms of direct ionization.

In extending the SCA method for these heavy projectiles, at $b = 0$, we use the united-atom binding energies, united-atomic radii, and as the velocity the collision velocity at $R = \infty$.

We concentrate on the excitation of the $2p\sigma$ MO, since most of the data pertain to it. The excitation probability according to SCA is given by

$$P_{2p\sigma} = \frac{2Z_P^2}{E_B} \mathcal{F}_{2p\text{III/II}}(x). \quad (6)$$

The function $\mathcal{F}(x)$ is given in the Tables of Hansteen *et al.*²⁷ and is plotted as a full line in Fig. 7. In order to compare the experimental data to this curve, we plot $P_{\text{expt}}^* E_B^{\text{UA}} / 2Z_P^2$ as a function of $x = 1.39(E_B^{\text{UA}} r_{2p}^{\text{UA}} / E_{\text{lab}})$ (E_B^{UA} is in keV, r_{2p} in fm, and E_{lab} in MeV/u). In Fig. 7 we display both our and other relevant data from literature for the $2p\sigma$ excitation in different collision systems with Ni ions. In those cases where the $P(b)$ curve still displayed some shape typical for rotational cou-

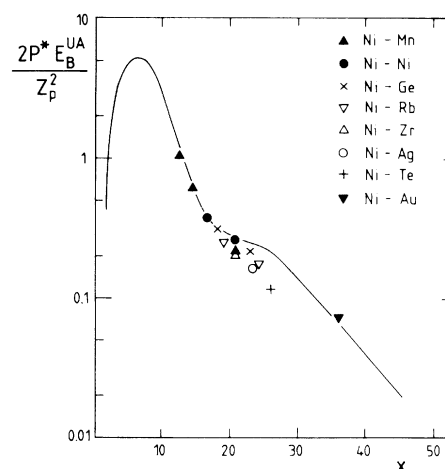


FIG. 7. Plot of the normalized plateau value at small impact parameters of the $2p\sigma$ vacancy-production probability in different collision systems with Ni projectiles vs $x = 1.39 E_B^{\text{UA}} r_{2p}^{\text{UA}} / E_{\text{lab}}$ (see explanation in text). The Ni-Mn data are from Ref. 23 and the Ni-Ni, Ni-Ge, and Ni-Rb data from Ref. 8.

pling, P_{expt}^* has been taken as the $P(b)$ value in the "valley" between the adiabatic and kinematic peaks. For all experimental data, the fluorescence yields given in Table I were used and the reduced outer electron screening (ΔE_{sc}) due to high ionization was taken into account with $\Delta E_{\text{sc}} = 2$ keV.

The rather amazing agreement in the absolute values between most experimental points and the calculated curve is certainly somewhat fortuitous considering the uncertainties; the agreement in the shape of the dependence on x is, however, more convincing, leading to the conclusion that the measured P_{expt}^* data can be explained by this "overstretched" SCA formalism, i.e., as direct excitation to the continuum.

This conclusion had already been proposed previously.²⁸ A plot of P_{expt}^* vs E_B^{UA} yields a $(E_B^{\text{UA}})^{-2}$ dependence which is in accordance with the systematic behavior of direct excitation.

Performing estimates according to the direct-ionization model of Briggs⁶ and Meyerhof,²⁵ taking for v the velocity of each perturbing potential in the center-of-mass system and using the SCA calculations of Ref. 27, one can again reproduce within a factor of 2 the absolute values of P_{expt}^* and their relative dependence on E_B^{UA} and the collision velocity.

Finally, it should be mentioned that the diffusion model used by Brandt and Jones²⁹ cannot explain the systematics found here experimentally for the excitation of inner shells in the different systems. The interaction radius R_0 —one of the parameters in the diffusion model—should approximately coincide with b_0 . On the other hand, according to the model, R_0 is a monotonously decreasing function of Z_T for fixed Z_P which contradicts even qualitatively the Ni→Au data.

IV. SUMMARY

In contrast to the symmetric Ni-Ni collision system, the impact-parameter dependences for Ni K excitation in the asymmetric systems Ni-Zr, Ni-Ag, Ni-Te, and Ni-Au do not display any feature of rotational coupling. The appearance of this coupling in the impact-parameter dependence depends on the availability of $2p\pi$ (in Au $3d\pi, \delta$) vacancies produced in the incoming part of the collision (see Fig. 2). When going from the symmetric Ni-Ni system to heavier targets, the target $2p$ binding-energy increases, and therefore the number of available $2p\pi$ vacancies decreases. This explains at least partly

why in the more symmetric Ni-Ge and Ni-Rb systems some indication of rotational coupling is still discernible,⁸ while in the increasingly asymmetric systems it disappears.

Hence, for the investigated asymmetric systems a direct excitation of the relevant MO at small internuclear distances is expected to be the dominant excitation mechanism and the resulting $P(b)$ curves have indeed shapes typical of direct excitation. However, in contrast to low- Z systems, the excitation probabilities are high—from a few percent to about 10%. Therefore, in heavy systems, even when rotational coupling is still expected to be operative, the contributions to $P(b)$ due to the two mechanisms should be comparable. Indeed, the direct excitation was already assumed to fill up the valley between the adiabatic and kinematic peaks in $P(b)$ curves of symmetric or nearly symmetric collision systems.

The maximal contribution to the vacancy-production cross section $2\pi bP(b)db$ comes from impact parameters $b_0 = Cr_{\text{ad}}^{\text{UA}}$ with $C = 1.23 \pm 0.05$, in accordance with the Bang-Hansteen scaling rule.^{21,22} $r_{\text{ad}}^{\text{UA}}$ is the adiabatic radius calculated using united-atom binding energies; these adiabatic radii are much smaller than the relevant shell radii in the systems investigated. All measured $P(b)$ curves have similar shapes and can be reduced to one common curve by scaling the vacancy-production probability with its plateau value at low impact parameters P^* and the impact parameter with $r_{\text{ad}}^{\text{UA}}$.

The dependence of the plateau probabilities P^* on target Z and collision velocity for all Ni→ Z_T measurements performed in this work and found in the literature could be described by an extension of the SCA method for calculating direct excitation, again using united-atom binding energies and shell radii.

In conclusion, the highest probable vacancy-production mechanism in these collisions is direct excitation from the molecular orbitals at small internuclear distances.

On the outgoing part of the collision the vacancies may be shared at large internuclear distances between adjacent inner orbitals. The data are consistent with an impact-parameter independent sharing probability w . Since this process is active up to much larger impact parameters than the direct ionization of the tighter bound shell it ends up, in those cases in which it is effective, having the dominant contribution to the total vacancy-production cross section.

- *Present address: Department of Physics, Technion, 32000 Haifa, Israel.
- †Present address: Hahn-Meitner Institut für Kernforschung, D-1000 Berlin 39, Federal Republic of Germany.
- ¹P. H. Mokler and F. Folkmann, in *Structure and Collisions of Ions and Atoms*, edited by I. A. Sellin (Springer, Berlin, 1978), p. 201.
- ²W. E. Meyerhof and K. Taulbjerg, *Annu. Rev. Nucl. Sci.* **27**, 279 (1977).
- ³D. Liesen, P. Armbruster, F. Bosch, S. Hagmann, P. H. Mokler, H. J. Wollersheim, H. Schmidt-Böcking, R. Schuch, and J. B. Wilhelmy, *Phys. Rev. Lett.* **44**, 983 (1980).
- ⁴F. Bosch, D. Liesen, P. Armbruster, D. Maor, P. H. Mokler, H. Schmidt-Böcking, and R. Schuch, *Z. Phys. A* **296**, 11 (1981).
- ⁵J. U. Andersen, E. Laegsgaard, M. Lund, and C. D. Moak, *Nucl. Instrum. Methods* **132**, 507 (1976).
- ⁶J. S. Briggs, *J. Phys. B* **8**, L485 (1975).
- ⁷K. Taulbjerg, J. S. Briggs, and J. Vaaben, *J. Phys. B* **9**, 1351 (1976).
- ⁸R. Schuch, G. Nolte, and H. Schmidt-Böcking, *Phys. Rev. A* **22**, 1447 (1980).
- ⁹G. Gaulker, H. Schmidt-Böcking, R. Schuch, R. Schule, H. J. Specht, and I. Tserruya, *Nucl. Instrum. Methods* **141**, 115 (1977).
- ¹⁰E. Storm and H. I. Israel, *Nucl. Data Tables* **A7**, 565 (1970).
- ¹¹J. S. Greenberg, P. Vincent, and W. Lichten, *Phys. Rev. A* **16**, 964 (1977).
- ¹²W. A. Schönfeldt, thesis, University of Köln, 1981, GSI Report No. 81-8 (unpublished).
- ¹³D. Maor, D. Liesen, P. H. Mokler, B. Rosner, H. Schmidt-Böcking, and R. Schuch, in *Inner Shell and X-Ray Physics of Atoms and Solids*, edited by J. Fabian, H. Kleinpoppen, and L. M. Watson (Plenum, New York, 1981), p. 67.
- ¹⁴J. Bang and J. M. Hansteen, *K. Dan. Vidensk. Selsk., Mat.-Fys. Medd.* **31**, 1 (1959).
- ¹⁵G. Nolte, J. Volpp, R. Schuch, H. J. Specht, W. Lichtenberg, and H. Schmidt-Böcking, *J. Phys. B* **13**, 4599 (1980).
- ¹⁶W. E. Meyerhof, *Phys. Rev. Lett.* **31**, 1341 (1973).
- ¹⁷W. Fritsch and U. Wille, *J. Phys. B* **12**, L645 (1979).
- ¹⁸R. Shanker, R. Bilau, R. Hippler, U. Wille, and H. O. Lutz, *J. Phys. B* **14**, 997 (1981).
- ¹⁹D. H. Jakubassa and K. Taulbjerg, *J. Phys. B* **13**, 757 (1980).
- ²⁰D. Trautmann and F. Rösel, *Nucl. Instrum. Methods* **169**, 259 (1980).
- ²¹J. Bang and J. M. Hansteen, *Phys. Lett.* **72A**, 218 (1979).
- ²²P. Armbruster, H.-H. Behncke, S. Hagmann, D. Liesen, F. Folkmann, and P. H. Mokler, *Z. Phys. A* **288**, 277 (1978).
- ²³D. Maor, B. Rosner, M. Meron, H. Schmidt-Böcking, and R. Schuch, *J. Phys. B* **14**, 693 (1981).
- ²⁴B. M. Johnson, K. W. Jones, W. Brandt, F. C. Jundt, G. Guillaume, and T. H. Kruse, *Phys. Rev. A* **19**, 81 (1979).
- ²⁵W. E. Meyerhof, *Phys. Rev. A* **18**, 414 (1978).
- ²⁶W. E. Meyerhof, *Phys. Rev. A* **20**, 2235 (1979).
- ²⁷J. M. Hansteen, O. M. Johnsen, and L. Kocbach, *At. Data Nucl. Data Tables* **15**, 305 (1975).
- ²⁸P. H. Mokler, P. Armbruster, F. Bosch, D. Liesen, D. Maor, W. A. Schönfeldt, H. Schmidt-Böcking, and R. Schuch, in *Inner Shell and X-Ray Physics of Atoms and Solids*, edited by D. J. Fabian, H. Kleinpoppen, and L. M. Watson (Plenum, New York, 1981), p. 49.
- ²⁹W. Brandt and K. W. Jones, *Phys. Lett.* **57A**, 35 (1976).